# Relationship Between Jaw Stiffness and Kinematic Variability in Speech

DOUGLAS M. SHILLER,[1] RAFAEL LABOISSIÈRE,[2,3] AND DAVID J. OSTRY[1,4]

[1]*McGill University, Montreal, Quebec H3A 1B1, Canada;* [2]*Max Planck Institute, 80799 Munich, Germany;* [3]*Institut de la Communication Parlée, 38031 Grenoble, France; and* [4]*Haskins Laboratories, New Haven, Connecticut, 06511*

**Shiller, Douglas M., Rafael Laboissière, and David J. Ostry.** Relationship between jaw stiffness and kinematic variability in speech. *J Neurophysiol* 88: 2329–2340, 2002; 10.1152/jn.00286.2002. Humans produce speech by controlling a complex biomechanical apparatus to achieve desired speech sounds. We show here that kinematic variability in speech may be influenced by patterns of jaw stiffness. A robotic device was used to deliver mechanical perturbations to the jaw to quantify its stiffness in the mid-sagittal plane. Measured jaw stiffness was anisotropic. Stiffness was greatest along a protrusion-retraction axis and least in the direction of jaw raising and lowering. Consistent with the idea that speech movements reflect directional asymmetries in jaw stiffness, kinematic variability during speech production was found to be high in directions in which stiffness is low and vice versa. In addition, for higher jaw elevations, stiffness was greater and kinematic variability was less. The observed patterns of kinematic variability were not specific to speech—similar patterns appeared in speech and nonspeech movements. The empirical patterns of stiffness were replicated by using a physiologically based model of the jaw. The simulation studies support the idea that the pattern of jaw stiffness is affected by musculo-skeletal geometry and muscle-force-generating abilities with jaw geometry being the primary determinant of the orientation of the stiffness ellipse.

## INTRODUCTION

Studies of human arm stiffness have influenced recent empirical and modeling work on motor control (Flash 1987; Flash and Mussa-Ivaldi 1990; Gomi and Kawato 1996; Gribble et al. 1998; Mussa-Ivaldi et al. 1985; Tsuji et al. 1995). In the present paper, we have taken a comparable approach to the study of motor control in the orofacial system. We provide direct measures and simulation studies of human jaw stiffness and assess the relationship between patterns of jaw stiffness and kinematic variability during speech production.

There is an extensive literature on the motor control of the jaw that focuses on the human masticatory system (for reviews, see Hannam and McMillan 1994; Hellsing 1987; Luschei and Goldberg 1981; Trulsson and Johansson 1996; van Eijden and Turkawski 2001; Wood 1987). This includes studies of motor-unit properties and afferent mechanisms as well as studies of jaw-movement kinematics, electromyographic activity, and force production. Little is known, however, about stiffness in the orofacial system. Stiffness is a measure of resistance to displacement and is affected by central neural inputs, reflexes, muscle properties, and the geometry of muscle attachments. Cooker et al. (1980) have measured human jaw stiffness during maintained bite force. Muller et al. (1984) have provided estimates of perioral stiffness based on mechanical perturbations to the lips during speech. In addition, inferences about stiffness in speech production have been made on the basis of kinematic measures (Kelso et al. 1985; Ostry and Munhall 1985).

Human jaw stiffness may affect kinematic variability in speech. In particular, stiffness may contribute to differences in variability in different movement directions. Because stiffness characterizes resistance to displacement, directions in which stiffness is high may exhibit less variability than directions in which stiffness is low. It may thus be the case that the pattern of variability in jaw position that accompanies the production of speech sounds reflects the directional asymmetries of stiffness of the jaw.

A relationship between stiffness and kinematic variation might be expected on the basis of patterns observed when subjects compensate for destabilizing loads to the limb (Milner 2002). The ability of subjects to compensate for these loads has been shown to depend on the direction of the perturbation relative to the shape of the stiffness field at the hand. Specifically, there is a greater effect on limb position when loads act in directions of lower stiffness and a smaller effect in directions of higher stiffness. Kinematic variation in speech production may be similarly dependent on the magnitude of jaw stiffness in different directions.

In the present paper, we report direct measures of jaw stiffness in the sagittal plane that were obtained by applying precise mechanical perturbations to the jaw at positions associated with the production of vowels. Jaw stiffness was found to be anisotropic, with higher stiffness observed along the axis of jaw protrusion and retraction. Patterns of kinematic variability were assessed for the same set of speech sounds and were shown to be related in a detailed manner to the directions and magnitudes of jaw stiffness. Simulation studies support the idea that the pattern of jaw stiffness arises from the balance of muscle-force-generating abilities and musculo-skeletal geometry in the orofacial system.

---

Address for reprint requests: D. J. Ostry, Dept. of Psychology, McGill University, 1205 Dr. Penfield Ave., Montreal, QC H3A 1B1, Canada (E-mail: ostry@motion.psych.mcgill.ca).

METHODS

Six subjects (4 males and 2 females) participated in the measurement of jaw stiffness. Measures of kinematic variability were obtained for the same subjects. None of the subjects reported any history of speech motor disorder or temporo-mandibular joint dysfunction. All experimental procedures used in the present study were approved by the Ethics Review Board of the Department of Psychology at McGill University.

### Measurement of jaw stiffness

Measures of jaw stiffness were obtained by connecting a computer-controlled robotic device (Phantom Premium 1.0, Sensable Technologies, Woburn, MA) to an acrylic and metal dental appliance that was attached to the mandibular teeth. The appliance was custom molded for each subject and glued to the buccal surface of the teeth using a dental adhesive (Iso-Dent, Ellman International, Hewlett, NY). The coupling between the robot and the jaw was achieved by using a magnesium and titanium rotary connector that permitted motion of the jaw in all six translational and rotational degrees of freedom. Subjects were thus able to produce naturalistic jaw movements when coupled to the robot (see Fig. 1).

The robot consisted of a cable-drive mechanism with encoders for position measurement (0.03-mm position resolution) and a six-axis ATI Nano-17 force/torque sensor (ATI Industrial Automation, Apex, NC), mounted on the tip of the robot, for measurement of subject applied forces. The robot was chosen because of its low inertia (less than 75 g apparent mass at the tip) and low friction in combination with its ability to produce force in all three spatial dimensions (3D).

The experiments were carried out with the head immobilized. This was achieved by connecting a second dental appliance that was attached to the maxillary teeth to a rigid metal frame. During the experiment, subjects were seated in a chair with the back of their head resting against a support. The head-restraint apparatus consisted of two articulated metal arms, one on each side of the head, that were locked in place during data collection.

Jaw position was sampled at 1,000 Hz. Jaw restoring forces were sampled at 100 Hz and then linearly interpolated to match the sampling rate of the position signal.

The subject's task was to maintain static jaw postures associated with the production of the four English vowels: /i/ as in "heat," /e/ as in "head," /a/ as in "cot," and /æ/ as in "cat." These vowels were selected to vary jaw elevation. While the subject maintained a static jaw position, small ramp-and-hold force perturbations (1 N, 50-ms rise time, 500-ms hold time) were applied. The perturbations were delivered in 16 directions spaced equally about a circle in the midsagittal plane (every 22.5°). The order of perturbations was random-

ized. A rest interval of 500 ms occurred between perturbations. Perturbations were blocked by vowel with the order of vowels randomized across subjects. For each subject, each of the four vowels was tested twice. We have limited perturbations to the sagittal plane because jaw motion in speech is essentially restricted to sagittal plane movement (Ostry et al. 1997).

To ensure that subjects maintained the same jaw position prior to each perturbation, visual feedback of jaw position was provided. Prior to a series of perturbations, the subject produced a sustained vowel for several seconds, at which point the 3D position of the jaw was measured and displayed on a computer screen located in front of the subject. A circle in the center of the computer display represented this desired position of the jaw, while another circle represented the jaw's current position. (The location of the circle on the display indicated the position of the jaw in the frontal plane. Circle diameter coded protrusion and retraction.) The subject was instructed to keep the jaw as close as possible to the desired position. Jaw perturbations were delivered only if the jaw was held stationary (tangential velocity less than 10 mm/s for 250 ms) at a distance of less than 1.5 mm from the desired position. Subjects were instructed to maintain the jaw position during the sequence of perturbations without voicing and to not voluntarily intervene (see *Data analysis*).

Pilot tests compared measures of stiffness that were obtained when voicing accompanied the perturbation with those obtained when subjects held the jaw at the same position in the absence of voicing. No differences in stiffness were observed under these conditions.

In pilot tests, estimates of jaw stiffness at the incisors were found to be similar for perturbations ranging from 1 to 3 N and for force rise times ranging from 25 to 100 ms. The 500-ms hold time during the perturbation was sufficient for the jaw to come to rest at the perturbed position.

### Measurement of jaw kinematic variability

Measures of jaw kinematic variability were obtained by tracking the motion of the head and jaw using Optotrak (Northern Digital, Waterloo, ON). This system records the 3D motion of infrared-emitting diodes (IREDs). To measure head motion, four IREDs were placed on a dental appliance that was attached to the maxillary teeth. Jaw movement was measured using four additional IREDs that were attached to an appliance on the mandibular teeth. The dental appliances had little effect on the intelligibility of the utterances tested in this study. IRED motion was measured at a sampling rate of 200 Hz.

Measures of jaw kinematic variability associated with vowel production were obtained from repetitions of simple speech sequences. Each sequence consisted of a consonant-vowel-consonant (CVC) combination that was embedded in a carrier sentence. Twelve CVC sequences were tested, resulting from the combination of the consonants /s/, /t/, and /k/ with the four vowels that were used in the measurement of jaw stiffness: /i/, /e/, /a/, and /æ/. The consonants were chosen to vary the jaw position at closure. The test sentences were of the form "say *ses*y again" or "say *tat*y again."

Subjects repeated each test sentence at a self-chosen rate and volume. Enough time was provided for subjects to produce 25 repetitions in each of the 12 experimental conditions. The order in which CVC combinations were tested was randomized across subjects.

### Data analysis

JAW STIFFNESS. Measures of position and force at the mandibular central incisors were transformed into a common head-centered coordinate system. The origin is at the tip of the maxillary incisors. The "horizontal" axis of this coordinate system is aligned with the occlusal axis (the positive direction corresponds to jaw protrusion). The vertical axis passes through the incisors and is orthogonal to the horizontal axis (jaw lowering is in the negative direction).

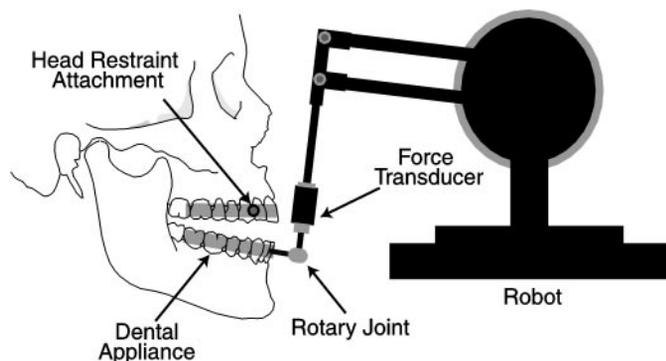A sample of the data from an individual perturbation is shown in



FIG. 1. Schematic of the experimental apparatus. An acrylic and metal dental appliance is used to attach the mandibular teeth to the robot. A similar appliance on the maxillary teeth provides a point of attachment to an external head restraint. A rotary joint connects the subject to the force transducer and provides unrestricted motion.

Fig. 2*A*. As force is applied by the robot, the jaw is displaced from its initial position. With the force held constant at 1 N, the jaw maintains a new static position. For purposes of data analysis, measures of jaw position and restoring force were averaged over two time windows, one immediately prior to the perturbation (25 ms) and one during the hold phase. The position and force measures during the hold phase were taken over a 100-ms interval, shown as ▨, that began 200 ms after the start of the perturbation. The difference between the two position values provides a measure of jaw displacement. The difference between the two forces gives a measure of restoring force related to the perturbation. The jaw's displacement and associated restoring force provide a measure of its spring-like behavior or stiffness. Because the jaw is essentially stationary at the displaced position, the contribution of viscosity and inertia may be neglected.

The example depicted in Fig. 2*A* is typical in that there is no voluntary movement in response to the perturbation. Jaw motion during the hold phase of the perturbation was negligible. Note that the magnitude of the force acting on the jaw is small, resulting in a net displacement of approximately 1 mm. In many cases subjects reported that the perturbations were barely perceptible.

Figure 2*B* shows an individual perturbation and the associated restoring force in the sagittal plane. A perturbation is delivered with the jaw initially at position [0, 0]. The perturbation causes the jaw to be displaced to a stationary final position at which time the position and restoring force are measured. The path followed by the jaw in response to the perturbation and the associated restoring force are both shown with dotted lines. The magnitude and direction of the perturbation and restoring force at steady state are represented as vectors (—).

Figure 2*C* illustrates the pattern of displacements and restoring forces at the mandibular incisors for perturbations in different direc-tions about a circle. The figure shows displacements (- - -) and in-wardly directed restoring forces (—) in the sagittal plane. A sample of only eight perturbations is shown, however in actual experiments 16 perturbation directions in the sagittal plane were used. Estimates of jaw stiffness are computed directly from this set of displacements and restoring forces.

Jaw stiffness in the sagittal plane—characterizing the relationship between force and jaw displacement measured at the tip of the mandibular incisors—is described by the following set of linear equations, adapted from Mussa-Ivaldi et al. (1985)

$$dF_x = -K_{xx}dx - K_{xy}dy \qquad (1)$$

$$dF_y = -K_{yx}dx - K_{yy}dy \qquad (2)$$

where $dF_x$ and $dF_y$ represent the horizontal and vertical components of the restoring force vector, $dx$ and $dy$ represent the displacement and $K$ is the stiffness matrix. $K_{xx}$ is the component of stiffness relating restoring force in $x$ to displacement in $x$, $K_{xy}$ relates restoring force in $x$ to displacement in $y$ and so forth. In matrix notation, these equations can be written as

$$\left[ \begin{array}{c} dF_x \\ dF_y \end{array} \right] = - \left[ \begin{array}{cc} K_{xx} & K_{xy} \\ K_{yx} & K_{yy} \end{array} \right] \left[ \begin{array}{c} dx \\ dy \end{array} \right] \qquad (3)$$

or

$$dF = -K \, dx \qquad (4)$$

For each subject, the values of the stiffness matrix were obtained by least-squares regression using the forces and displacements associated with 32 mid-sagittal perturbations (2 repetitions of 16 perturbation directions) at each of the four vowel positions.
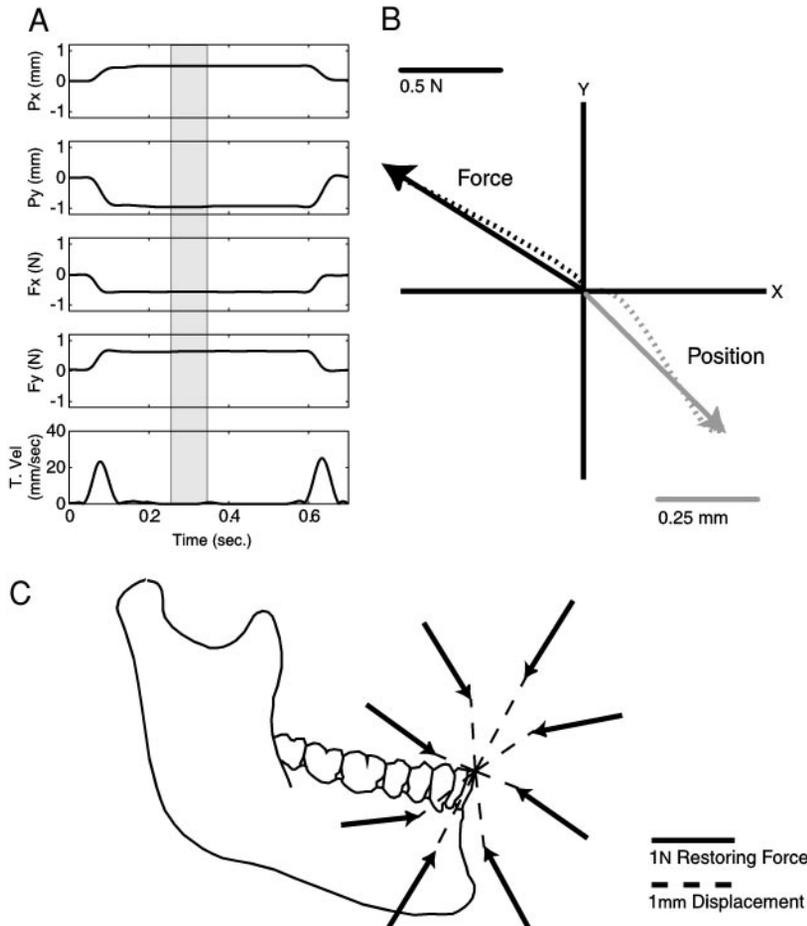


FIG. 2. *A*: measured restoring forces and jaw positions during the course of a perturbation. *Px* and *Py* indicate displacements in the horizontal and vertical directions resulting from the perturbation. *Fx* and *Fy* correspond to restoring forces. *T. Vel.* indicates the tangential velocity of the jaw. ▨, the time window over which data are averaged for the estimation of stiffness. *B*: instantaneous jaw position and restoring force over the course of a perturbation ( · · · ). Position and force change during the hold phase are shown as vectors. *C*: pattern of displacements (- - -) and restoring forces (vectors) for a set of perturbations in the sagittal plane. Note that the displacements are exaggerated with respect to the schematic of the jaw for purposes of display.

In a purely spring-like system, the off-diagonal terms of the stiffness matrix ($K_{xy}$ and $K_{yx}$) are equal in magnitude (that is, the matrix is symmetrical). The estimates of jaw stiffness in the present study essentially satisfy this condition (see RESULTS). Following Mussa-Ivaldi et al. (1985), each estimate of jaw stiffness was decomposed into a symmetric ($K_s$) and an antisymmetric ($K_a$) component. Only the symmetric component of stiffness was used in subsequent analyses. The decomposition of the stiffness matrix was carried out as follows

$$K_s = \begin{bmatrix} K_{xx} & \frac{1}{2}(K_{xy} + K_{yx}) \\ \frac{1}{2}(K_{yx} + K_{xy}) & K_{yy} \end{bmatrix} \quad (5)$$

$$K_a = \begin{bmatrix} 0 & \frac{1}{2}(K_{xy} - K_{yx}) \\ \frac{1}{2}(K_{yx} - K_{xy}) & 0 \end{bmatrix} \quad (6)$$

where $K = K_s + K_a$. In RESULTS, it is shown that the contribution to variance of the antisymmetric component of the stiffness matrix is neglectable.

The values of the stiffness matrix can be easily interpreted when represented graphically as an ellipse (see Fig. 3, *A* and *B*). The stiffness ellipse shows the predicted restoring force in each direction that results from a displacement of unit amplitude. The major axis of the ellipse defines the direction and magnitude of maximum stiffness. Similarly, the minor axis defines the direction and magnitude of least stiffness.

A number of quantitative measures were used to characterize jaw stiffness. The direction of maximum stiffness is the angle between the major axis of the stiffness ellipse and the horizontal axis (shown as $\theta$ in Fig. 3*B*). Values for maximum and minimum stiffness correspond to the magnitude of the ellipse along the major and minor axes. A global measure of the magnitude of stiffness was obtained by computing the area of the ellipse. Note that eigenvalues and eigenvectors of the stiffness matrix give the magnitude and orientation of the major and minor axes of the ellipse.

KINEMATIC VARIABILITY.    The 3D position data for each IRED were digitally low-pass filtered using a second-order zero phase lag Butterworth filter with a cutoff frequency of 10 Hz. The IRED motions were transformed into a six dimensional rigid-body representation of jaw position and orientation in head-centered coordinates (see Ostry et al. 1997, for details). The origin of this new coordinate system is at the tip of the maxillary incisors in the mid-sagittal plane. The "horizontal" axis is aligned with the occlusal plane. Consistent with the measures of jaw stiffness, data analysis of jaw motion was restricted to vertical and horizontal position in the sagittal plane.

An interactive computer program was used to identify the jaw position associated with the production of the vowel within each CVC. In the kinematic record, CVC production is typically associated with a relatively large-amplitude opening and closing movement of the jaw corresponding in time to the voiced portion of the CVC utterance. The position of maximum opening during the CVC was taken to be the position of the jaw during vowel production.

For each subject, the pattern of jaw kinematic variability associated with vowel production was examined separately for each of the 12 CVC conditions (4 vowels × 3 consonants). On the basis of the jaw position data, a 95% confidence ellipse was computed using principle components analysis (see Fig. 3*C*). The orientation and magnitude of the major axis of the ellipse corresponds to the direction and magnitude of maximum kinematic variability. The minor axis shows the direction and magnitude of minimum kinematic variability.

The direction of maximum kinematic variability was measured as the angle between the major axis of the ellipse and the horizontal axis (Fig. 3*D*). Values for maximum and minimum kinematic variability correspond to the magnitude of the major and minor axes. A global measure of the magnitude of kinematic variability was obtained by computing the area of the ellipse.

Three different consonants were used in the test utterances to provide a number of estimates of kinematic variability. For purposes of analysis, measures of kinematic variability for each subject were averaged across the three consonant conditions, providing a single measure of the magnitude and orientation of kinematic variability for each of the four vowel conditions. (There were no systematic differences in the patterns of kinematic variation among the 3 consonant conditions.)

*Simulation studies*

The simulations were based on a model of sagittal plane jaw and hyoid movement (Laboissière et al. 1996). The model includes seven muscle groups corresponding to anterior temporalis, posterior temporalis, lateral pterygoid, masseter, anterior digastric, posterior digastric, and sternohyoid (Fig. 4*A*). These muscle groups contribute to motion in four kinematic degrees of freedom: horizontal jaw position, sagittal plane jaw orientation (about an axis through the center of the mandibular condyle), horizontal hyoid position, and vertical hyoid position. The model includes neural control signals, position- and velocity-dependent reflexes, muscle mechanical properties, and jaw and hyoid bone dynamics.

The muscle mechanical model includes force generation due to the contractile element (the dependence of force on muscle length and velocity), activation dynamics due to calcium kinetics, and the passive dependence of force on muscle length (see Fig. 4*B*).

Modeled muscle geometry and anthropometrics are taken from anatomical sources (McDevitt 1989; Scheideman et al. 1980). The reader is referred to Shiller et al. (1999; 2001) and Ostry et al. (1996) for previous studies in which the jaw model was used.

In the model, control signals to jaw muscles are based on the $\lambda$ version of the equilibrium point (EP) hypothesis. Jaw position is determined by centrally specified values of the muscle lengths at which motoneuron recruitment begins ($\lambda$). Through the coordination of $\lambda$ values associated with individual muscles, different equilibrium positions and different levels of muscle cocontraction can be achieved (for a detailed description of the EP formulation, see Feldman et al. 1990).

In the context of the present experiment, restoring forces are measured with the jaw stationary. Under these conditions, modeled muscle force resulting from muscle activation is given by

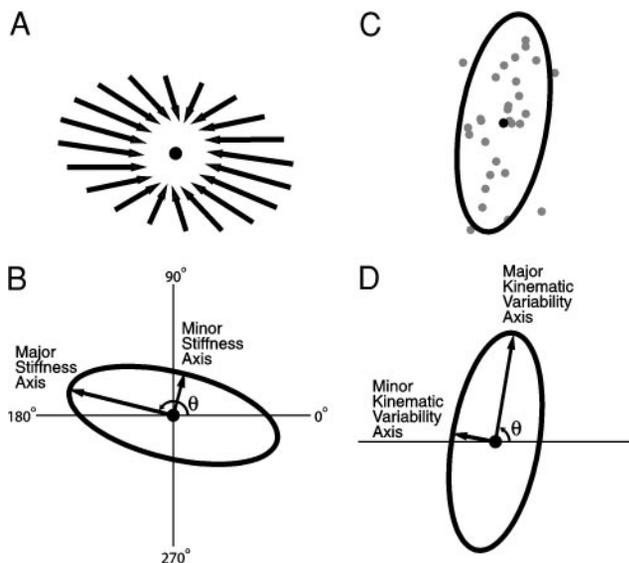$$M = \rho[\exp(c[x - \lambda]^+) - 1] \quad (7)$$



FIG. 3.    *A*: restoring force vectors predicted from the symmetric stiffness matrix on the basis of unit displacements in directions about a circle. *B*: orientation of the major axis of the stiffness ellipse ($\theta$) is defined relative to the horizontal. *C*: a 95% confidence ellipse is fit to measures of jaw position during vowel production. *D*: the orientation of the kinematic variability ellipse ($\theta$) is defined relative to the horizontal axis.
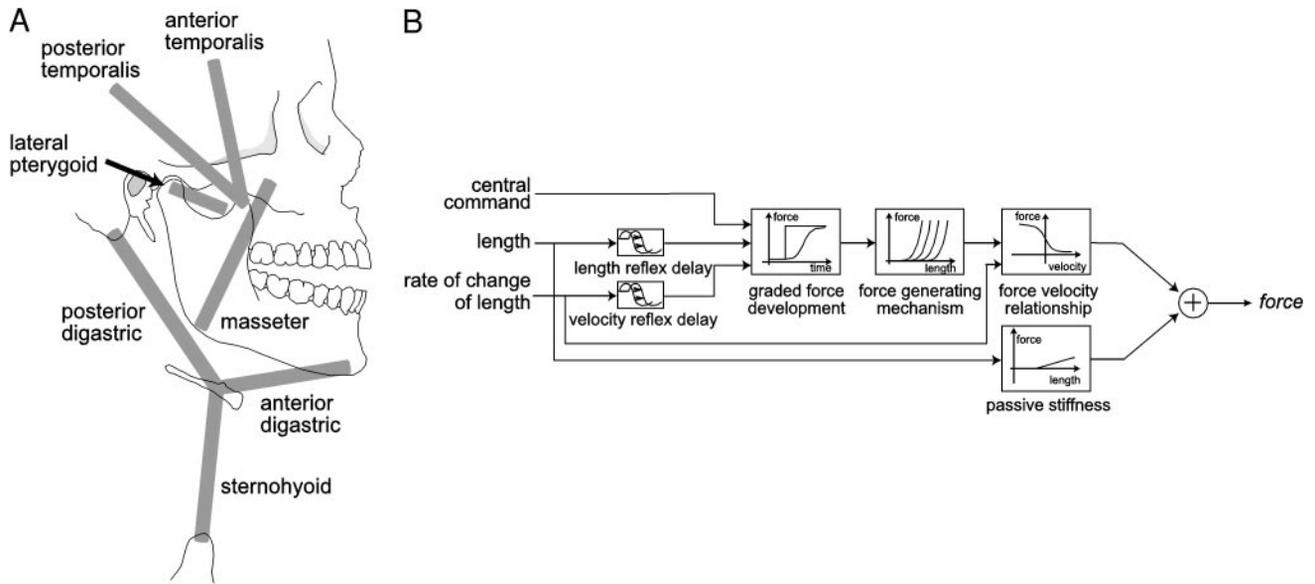
FIG. 4. *A*: schematic showing modeled muscles and attachments. *B*: muscle model used in the simulations includes the dependence of force on length and velocity, the graded development of force over time, passive stiffness, position- and velocity-dependent afferent inputs, and central input.

where

$$[x]^+ = \begin{cases} x, & \text{if } x > 0 \\ 0, & \text{if } x \leq 0 \end{cases} \qquad (8)$$

$M$ is steady-state active muscle force, $\rho$ is a magnitude parameter related to muscle force-generating ability, $c$ is a form parameter related to the shape of the force-length relationship (assumed to be the same for all muscles), $x$ is the current muscle length, and $\lambda$ is the centrally specified threshold length. Values for $\rho$ are based on estimates of maximum muscle force and physiological cross sectional area (McGrath and Mills 1984; Mills et al. 1988; Pruim et al. 1980; Weir and Abrahams 1978).

## RESULTS

### *Measures of jaw stiffness*

Sagittal plane jaw stiffness was estimated for each subject separately at each of the four vowel positions. Figure 5*A*, shows stiffness ellipses for two subjects. The position of the jaw during the perturbations is shown with a filled circle in the center of each ellipse. The ellipses show stiffness for the vowels /i/ (top), /e/, /a/, and /æ/ (bottom). It may be seen that jaw stiffness is anisotropic with higher stiffness in the direction of jaw protrusion and retraction and lower stiffness in the direction of raising and lowering. Little change is observed in the orientation of the ellipse depending on the position of the jaw. A small but consistent difference in the overall magnitude of stiffness accompanies differences in the elevation of the jaw. Stiffness is greater in magnitude for the highest vowel position (associated with the production of /i/) than for lower jaw positions. This pattern of results was observed in all subjects.

Jaw-stiffness estimates are presented for all subjects separately in Table 1. Values are given as elements of the stiffness matrix. The associated eigenvalues that define the magnitudes of the major and minor axes of the stiffness ellipse range from
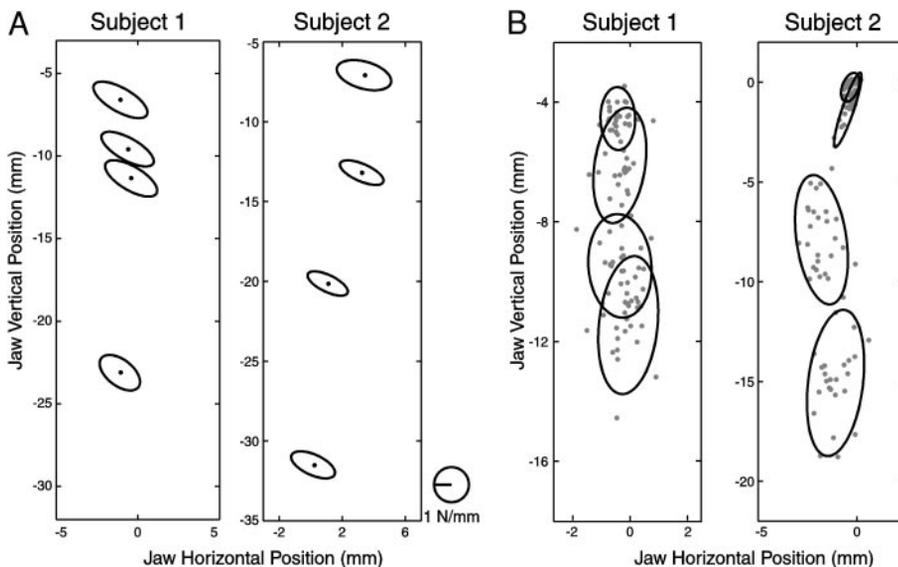


FIG. 5. *A*: jaw-stiffness ellipses for 2 subjects. ●, the position of the mandibular incisors for the 4 vowel conditions. Stiffness is greater along the axis of protrusion and retraction (see RESULTS for details). *B*: kinematic variability ellipses for the same 2 subjects. Raw data points and 95% confidence ellipses are shown. Variability is greatest along the axis of jaw raising and lowering.

1.37 to 2.03 N/mm on the major axis and 0.27 to 1.15 N/mm on the minor axis. Jaw stiffness at the incisors is thus two to four times larger than stiffness of the human arm (measured at the hand) (Mussa-Ivaldi et al. 1985; Tsuji et al. 1995).

Repeated-measures ANOVA was used to assess differences between vowels in the orientation of the major axis of the stiffness ellipse. No reliable statistical differences in orientation were observed. The mean orientation of the major axis with respect to the occlusal plane was 164.4, 159.4, 159.8, and 159.2° for /i/, /e/, /a/, and /æ/, respectively. The mean orientation across all conditions was 160.7° and ranged from 148.3 to 169.6° across subjects. Figure 6A (thick lines) shows the mean ellipse orientation for each subject as a small vector and the overall average orientation as a large vector.

Differences in the magnitude of stiffness were also assessed using ANOVA. Analyses were carried out for both the major and minor axes (Fig. 7A, *top 2 panels*) and on the overall area of the ellipse (Fig. 7B, thick line). The magnitude of stiffness on the major axis of the ellipse was found to be significantly greater than the stiffness on the minor axis ($P < 0.01$). This pattern was true of all subjects and all experimental conditions. Jaw stiffness also differed among the four vowel conditions ($P < 0.01$). Tukey tests of pairwise differences revealed greater stiffness on the major axis for the position associated with the high vowel /i/ than for the low vowels /a/ and /æ/ ($P < 0.05$). On the minor axis, the magnitude of stiffness was found to be greater for the position for /i/ than for /e/ and /a/ ($P < 0.01$). No differences in jaw stiffness were observed between the mid and low jaw positions corresponding to the vowels /e/, /a/, and /æ/. An examination of the area of the stiffness ellipse—a measure that reflects the total magnitude of jaw stiffness—revealed a comparable pattern of differences between vowels. Ellipse area was greater for the highest vowel position than for each of the three lower vowels ($P < 0.01$).

### Reliability of stiffness estimate

The computation of the jaw-stiffness matrix involves a least-squares regression that relates jaw restoring force to displacement. The resulting matrix is decomposed into symmetric and anti-symmetric components of which only the symmetric com-

ponent is used in subsequent analysis. The extent to which the symmetric stiffness matrix successfully captures the empirical pattern of variation was quantified using an $R^2$ measure of goodness-of-fit. This measure was obtained separately for each subject and each vowel tested. The computation involved the use of measured force levels and those predicted by the symmetric stiffness matrix. Specifically

$$R^2 = 1 - \frac{\Sigma (F - F')^2}{\Sigma (F - \bar{F})^2} \qquad (9)$$

where $F$ is a matrix of measured forces, $F'$ is a matrix of predicted forces obtained by using the symmetric stiffness matrix, and $\bar{F}$ is the mean of measured forces. The summation ($\Sigma$) is applied over all horizontal and vertical values of force. It was found that, on average, the proportion of variance accounted for by the symmetric stiffness matrix was 93% ($R^2 = 0.93$), ranging from 81 to 97% across subjects.

The anti-symmetric (curl) component of the stiffness matrix is a measure of deviation from purely spring-like behavior. In the present study, the magnitude of the anti-symmetric component of the stiffness matrix was on average very small in comparison to the symmetric stiffness component. The mean curl (computed as one-half of the difference between the off-diagonal components of the stiffness matrix) was 0.041 N/mm, approximately 2% of the maximum eigenvalue (1.682 N/mm) of the symmetric stiffness matrix and 6% of the minimum eigenvalue (0.717 N/mm). Furthermore, on average, only 1% of variance in the empirical data were accounted for by the anti-symmetric stiffness component ($R^2 = 0.013$). The relatively small contribution of curl to the measure of stiffness indicates that the neuromuscular system of the jaw exhibits primarily spring-like behavior in response to small amplitude perturbations.

### Measures of kinematic variability

Patterns of jaw kinematic variability are illustrated in Fig. 5B for the same two subjects as in Fig. 5A. Variability ellipses are shown for the vowels /i/ (top), /e/, /a/, and /æ/ (bottom). Jaw kinematic variability is observed to be anisotropic for all vow-

TABLE 1. *Estimated jaw stiffness matrix* $\begin{bmatrix} K_{yy} & K_{yx} \\ K_{xy} & K_{xx} \end{bmatrix}$

| Subject | /i/ | | /e/ | | /a/ | | /æ/ | |
|---|---|---|---|---|---|---|---|---|
| *1* | −0.5031 | −0.3812 | −0.4835 | −0.4477 | −0.5148 | −0.3660 | −0.6208 | −0.3176 |
| | −0.3508 | −1.4420 | −0.5347 | −1.3840 | −0.4858 | −1.1524 | −0.5565 | −1.3223 |
| *2* | −1.0695 | −0.2801 | −0.9838 | −0.2544 | −0.8521 | −0.3224 | −0.8984 | −0.3074 |
| | −0.3136 | −1.7220 | −0.3860 | −1.4988 | −0.3005 | −1.5870 | −0.2721 | −1.5575 |
| *3* | −1.1562 | −0.5022 | −1.0970 | −0.5143 | −1.1510 | −0.4876 | −1.1287 | −0.1916 |
| | −0.5995 | −1.4210 | −0.5711 | −1.3705 | −0.5665 | −1.3703 | −0.4457 | −1.0999 |
| *4* | −1.1794 | −0.1867 | −1.0036 | −0.2598 | −0.7619 | −0.2393 | −0.9647 | −0.1786 |
| | −0.1096 | −2.0026 | −0.2191 | −1.5988 | −0.1296 | −1.6261 | −0.1659 | −1.8236 |
| *5* | −0.9507 | −0.2555 | −0.7377 | −0.3342 | −0.7304 | −0.3094 | −0.8287 | −0.3093 |
| | −0.3254 | −1.6709 | −0.4266 | −1.2921 | −0.4303 | −1.1863 | −0.3941 | −1.3088 |
| *6* | −1.1114 | −0.0601 | −0.8070 | −0.1418 | −0.7539 | −0.2079 | −0.8101 | −0.1957 |
| | −0.0729 | −1.8833 | −0.1622 | −1.7161 | −0.2723 | −1.6892 | −0.2518 | −1.7629 |

Values for jaw stiffness. The *Y* axis corresponds to the vertical direction. The *X* axis corresponds to the horizontal direction. Note that in this table alone, the negative *X* direction corresponds to jaw protrusion.
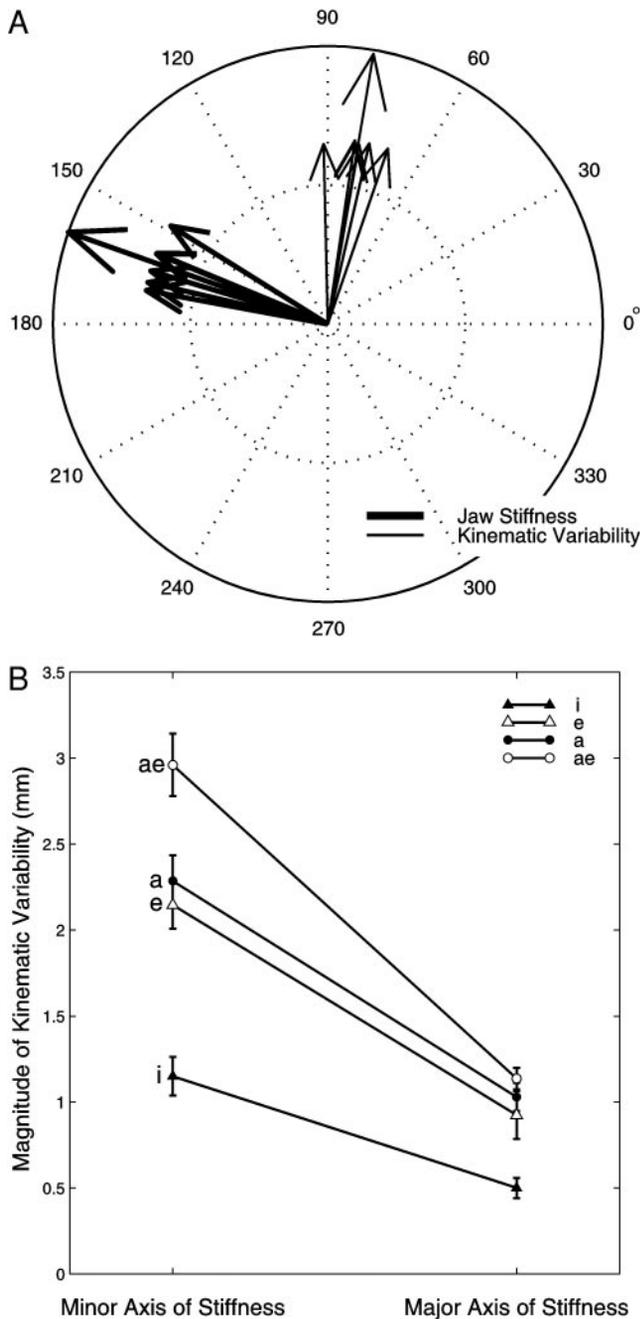
FIG. 6. *A*: orientation of the major axes of the stiffness and kinematic variability ellipses. Individual subject means are shown as small vectors. The grand means are shown with large vectors. *B*: kinematic variability measured in the direction of the major and minor axes of the stiffness ellipse. Values are averaged across subjects; ±SE is shown. In all cases, kinematic variability is less in the direction of maximum stiffness than in the direction of minimum stiffness.

the major axis of the kinematic variability ellipse was 74.0, 80.3, 85.2, and 81.9° for /i/, /e/, /a/, and /æ/, respectively. The mean orientation across all conditions was 80.4°, ranging from 70.9 to 91.3° across subjects (see Fig. 6*A*, thin lines).

ANOVA was also used to assess differences in the magnitude of kinematic variability. Analyses examined the magnitudes of the major and minor axes (Fig. 7*A*, *bottom 2 panels*) and the area of the kinematic variability ellipse (Fig. 7*B*, thin line). Variability on the major axis of the ellipse was consistently greater than variability on the minor axis ($P < 0.01$). The magnitude of the major and minor axes also varied across the four vowel conditions ($P < 0.01$). For the major axis, Tukey tests indicated that kinematic variability was less for the high vowel /i/ than for the three lower vowels /e/, /a/, and /æ/ ($P < 0.01$). Furthermore, kinematic variability for the mid-vowel /e/ was less than for the lowest vowels /a/ ($P < 0.05$) and /æ/ ($P < 0.01$). On the minor axis, variability was less for /i/ than for the
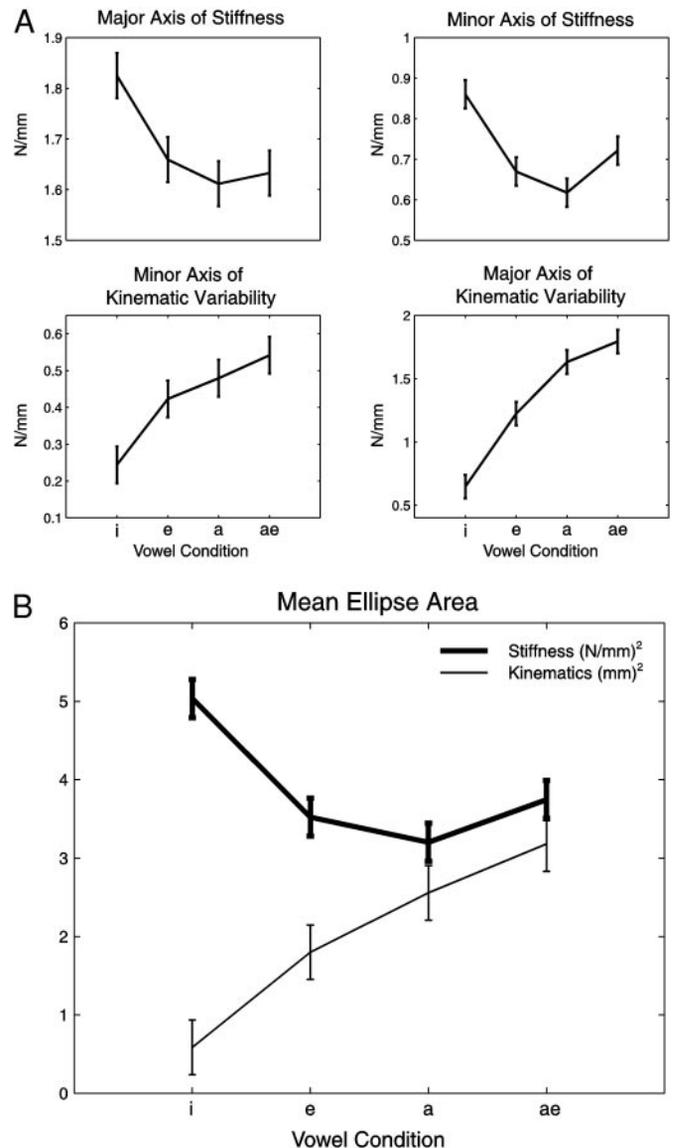


FIG. 7. *A*: magnitudes of stiffness and kinematic variability along the major and minor axes of the ellipses. Values for different vowel conditions averaged over subjects are shown. Error bars indicate ±SE. *B*: area of stiffness and kinematic variability ellipses averaged over subjects. The pattern of stiffness mirrors the pattern of kinematic variability.

els. The pattern is opposite to that observed for jaw stiffness—variability is greater along an axis of jaw raising and lowering and less along an axis of jaw protrusion and retraction. There is an effect of workspace position on the magnitude of kinematic variability. Variability is less for the high vowel than for the lower vowels. This basic pattern was shown by all subjects.

ANOVA was used to assess differences in the orientation of the kinematic variability ellipses between vowels. There were no reliable differences in orientation. The mean orientation of

low vowels /a/ ($P < 0.05$) and /æ/ ($P < 0.01$). No reliable differences were observed among the vowels /e/, /a/, and /æ/. An examination of the overall area of the variability ellipse indicated that there was less variability for /i/ than for each of the three lower vowels ($P < 0.01$). Variability for /e/ was less than for /a/ ($P < 0.05$) and /æ/ ($P < 0.01$).

### Relationship between stiffness and kinematic variability

To the extent that differences in jaw kinematic variability arise due to differences in stiffness, it would be expected that variability would be low in directions in which stiffness is high and that variability would be high when stiffness is low. Figure 6A shows the overall mean directions of maximum stiffness and maximum kinematic variability. Individual subject means are shown as smaller vectors. The directions of maximum stiffness and maximum kinematic variability are nearly orthogonal (80.3°), which is consistent with the idea that variability is dependent on differences in stiffness.

To quantitatively assess the relationship between stiffness and kinematic variability, we have examined the magnitude of kinematic variability in the direction of the major and minor axes of the stiffness ellipse. This was done for each subject and each vowel separately. Figure 6B shows the average magnitude of kinematic variability in the direction of maximum and minimum stiffness. The pattern is shown for each of the four vowels separately. Overall, variability is less in the direction of maximum stiffness than in the direction of minimum stiffness ($P < 0.01$). Tukey tests indicated that this pattern was reliable for each of the four vowel conditions ($P < 0.01$).

A relationship between jaw stiffness and kinematic variability may also be observed in terms of differences between high and low vowels. High vowels are associated with higher levels of stiffness and lower levels of kinematic variability. Low vowels display greater variability and lower stiffness. Figure 7B shows the mean area of the stiffness and kinematic variability ellipses for each of the four vowel conditions—measures that reflect the total magnitude of stiffness and variability. It may be seen that the pattern of jaw stiffness mirrors the pattern of jaw kinematic variability. The measure of stiffness is high when variability is low and vice versa. This relationship was examined quantitatively by computing a correlation coefficient relating stiffness and variability area measures using individual subject means for each vowel condition. A significant negative correlation was obtained ($P < 0.01$). A comparable relationship between stiffness and kinematic variability may be seen by examining the magnitudes of the individual axes of the stiffness and kinematic variability ellipses (see Fig. 7A).

### Kinematic variability under nonspeech conditions

To assess whether observed patterns of jaw kinematic variability were specific to speech, all subjects carried out an additional set of control tasks that consisted of jaw movements that were not associated with speech production. In one task, subjects were instructed to move their jaw repeatedly between a low elevation (corresponding to the workspace position for the vowel /æ/) and one of two higher jaw elevations (corresponding to the jaw position for /i/ or /e/). In a second task, subjects produced a series of jaw-protrusion movements initi-

ated from one of two initial jaw positions (corresponding to the jaw position for the vowels /i/ and /e/). The control studies were in all cases carried out prior to the tests involving speech.

In the task that involved primarily vertical movements, subjects moved between the two positions continuously at either a slow rate (approximately 0.5 Hz) or a fast rate (approximately 3 Hz). Enough time was allowed in each condition to collect 25 cycles. Movements were scored in a manner similar to that used for the study of jaw kinematic variability during speech production (see METHODS). Zero-crossings in jaw velocity were used to obtain positions for maximum and minimum jaw elevation. On the basis of these data points, the pattern of kinematic variability was characterized separately for the high and low (or medium and low) positions using a 95% confidence ellipse.

In the task involving jaw protrusion, subjects produced 25 individual movements (noncyclical) at either a fast rate (approximately 400 ms) or a slow rate (approximately 800 ms) initiated from one of the two starting positions. Movement amplitude along the horizontal axis averaged 7.5 mm across subjects. Jaw-protrusion movements were scored in a manner similar to that described for the vertical movements above. Zero crossings in jaw velocity were used to obtain positions for the most protruded position. 95% confidence ellipses were computed from this set of data points.

Figure 8A shows data from a single subject in the vertical movement condition (moving between the high and low position). For both positions, kinematic variability was found to be greater along an axis of jaw raising and lowering—the same pattern as that observed in speech movements. Figure 8C shows the pattern across subjects. The small vectors indicate the mean orientation of the major axis of the ellipse for each of the experimental conditions (3 jaw elevations × 2 movement speeds). The grand mean is shown as a large vector. The overall mean orientation (86.5°) is similar to that observed in the speech condition (80.4°).

Figure 8B shows data from the same subject in the jaw-protrusion task. The ● shows the mean initial jaw position; the variability ellipse at the protruded position is shown to the right. As in the case of vertical jaw movements, the magnitude of kinematic variability is greater in the direction of jaw raising and lowering. Figure 8D shows as small vectors the mean ellipse orientation across subjects for each of the four conditions (2 initial positions × 2 movement speeds). The overall mean orientation for the protrusion movements, shown as a large vector, is 85.9°, which is again similar to that observed in speech.

ANOVA was used to test the reliability of differences in ellipse orientation across conditions. In the vertical movement task, small but significant differences in the orientation of the kinematic variability ellipses were observed across the three jaw elevations ($P < 0.05$). In contrast, the manipulation of movement speed had no significant effect on the observed orientation. In the jaw-protrusion task, no reliable differences in ellipse orientation were found.

ANOVA was also used to test differences in the magnitude of kinematic variability. Values were obtained by computing the mean area of the kinematic variability ellipses. In the task involving vertical movement, ellipse area was found to vary among the three jaw elevations ($P < 0.01$). Tukey tests revealed that, as in the speech conditions, the magnitude of
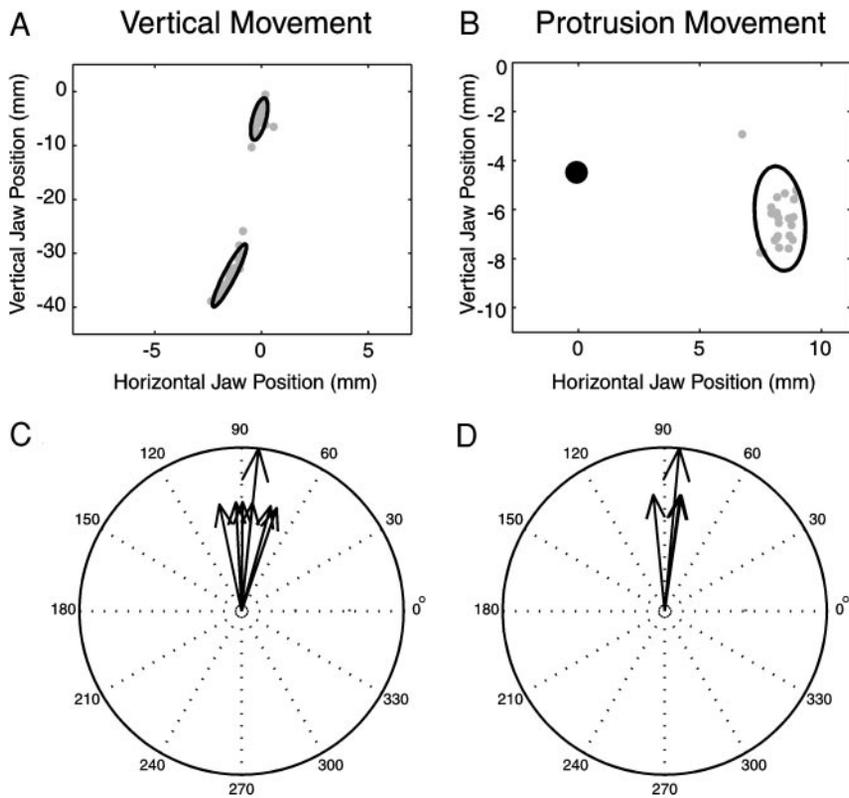
FIG. 8. Kinematic variability under nonspeech conditions. *A*: example of kinematic variability ellipses for movements between high and low jaw positions; 95% confidence ellipses and individual data points are shown. *B*: example of a kinematic variability ellipse for fast (approximate 400-ms duration) jaw-protrusion movements. ●, the mean initial position. *C*: orientation of the major axis of the ellipses for the vertical movement task. The small vectors show mean orientations for all amplitude and rate combinations. The large vector indicates the overall mean. *D*: ellipse orientation for the jaw-protrusion task. The small vectors show mean values for all rate and initial position combinations. The large vector shows the overall mean.

kinematic variability was less for the highest jaw elevation than for the lowest elevation ($P < 0.01$; Fig. 9). Ellipse area was also found to vary between the two movement speeds ($P < 0.05$). For the slower movement speed, the mean ellipse area was on average 34% less than the area for the fast movement speed. A similar pattern was observed for the jaw-protrusion task—variability was less for movements initiated from a
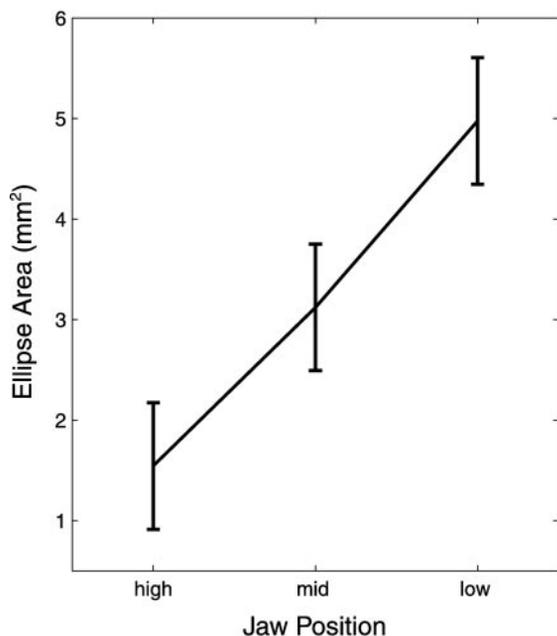


FIG. 9. In the nonspeech task involving vertical movements, the area of the kinematic variability ellipse varies systematically as a function of jaw position. Kinematic variability is less for the high jaw position than for the low position. ±SE is shown.

higher jaw position ($P < 0.05$). No differences in variability related to movement speed were observed.

### Simulations

The goal of the simulations was to assess the extent to which observed pattern of jaw stiffness might be accounted for by central commands (including coactivation), jaw muscle properties and musculo-skeletal geometry. In the simulations, we repeated the procedure carried out empirically to estimate jaw stiffness, holding constant modeled control signals that specify the position of the jaw. A series of simulated ramp-and-hold force pulses (1N, 50-ms rise time, 500-ms hold time) was applied to the jaw model in 16 equally spaced directions in the sagittal plane. As in the empirical study, the resulting displacements and restoring forces predicted by the model were used to compute estimates of stiffness.

The simulations were carried out with the jaw equilibrium angle held constant at 1, 4, or 7° relative to occlusion. This resulted in mandibular incisor positions that were approximately 2, 8, and 14 mm, again relative to occlusion. A modeled coactivation level of 10 N (total muscle force) was used.

When modeled control signals for jaw position were held constant, we obtained a pattern of jaw stiffness from the simulations that was similar to that observed empirically (Fig. 10*A*). At all three jaw positions, predicted jaw stiffness was anisotropic, such that stiffness was greater in the direction of jaw protrusion and retraction and less in the direction of jaw raising and lowering. The magnitude of stiffness on the major axis of the ellipse varied from 1.30 to 1.37 N/mm as a function of jaw elevation, and the magnitude of stiffness on the minor axis was 0.25–0.29 N/mm. These values are at the lower end
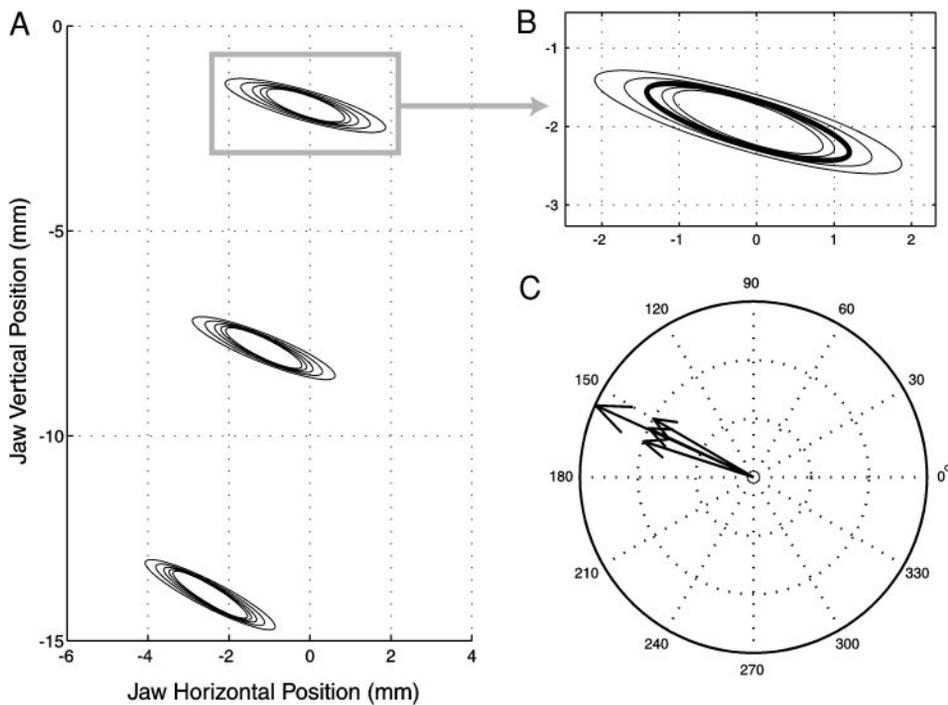
FIG. 10. *A*: simulated jaw-stiffness ellipses at 3 jaw positions. Ellipses are shown for modeled cocontraction levels ranging from 5 to 20 N. At each jaw position, stiffness is greater for higher cocontraction levels. *B*: detail of *A*. The thick line shows the stiffness ellipse at a cocontraction level of 10 N. *C*: orientation of the major axis of the stiffness ellipse averaged across cocontraction levels. Small vectors show mean orientations for each jaw position. The overall mean is shown as a large vector.

of the range observed in the subjects that were tested empirically.

Jaw stiffness is presumably affected by the level of muscle coactivation. Using the model, we explored the sensitivity of predicted stiffness to simulated coactivation levels that ranged from 5 to 20 N total muscle force ($-50$ to $+100\%$ of the value of 10 N that was used in the preceding simulations). Figure 10*B* shows that the level of coactivation has a systematic effect on jaw stiffness. A coactivation level of 5 N resulted in a reduction in the area of the stiffness ellipse of approximately 30% (inner most ellipse in Fig. 10*B*). A coactivation level of 20 N led to an increase in stiffness of approximately 50% (outer most ellipse). Changes in coactivation had little effect on the orientation of the stiffness ellipse.

Figure 10*C* shows the direction of the major axis of the simulated stiffness ellipses for the three jaw elevations (small vectors) averaged across cocontraction levels. The overall mean direction is shown as a larger vector. The mean orientation of the stiffness ellipses in the simulation was 156°. This value is quite close to that observed empirically (160.7°).

In work on human arm movement, limb geometry has been shown to be a primary determinant of the shape and orientation of the stiffness field at the hand. In the context of the present study, we have explored the role of jaw geometrical factors by systematically manipulating the shape of the modeled jaw and repeating the procedure for stiffness estimation. In particular, we altered the length of the three numbered segments in Fig. 11*A* that contribute to the anthropometry of the jaw in the sagittal plane. The length of each segment was altered by up to $\pm50\%$ either one segment at a time, or in pairs. The simulations were carried out with the jaw at an elevation of 4° relative to occlusion, using a cocontraction level of 10 N. The changes in jaw geometry were found to have a
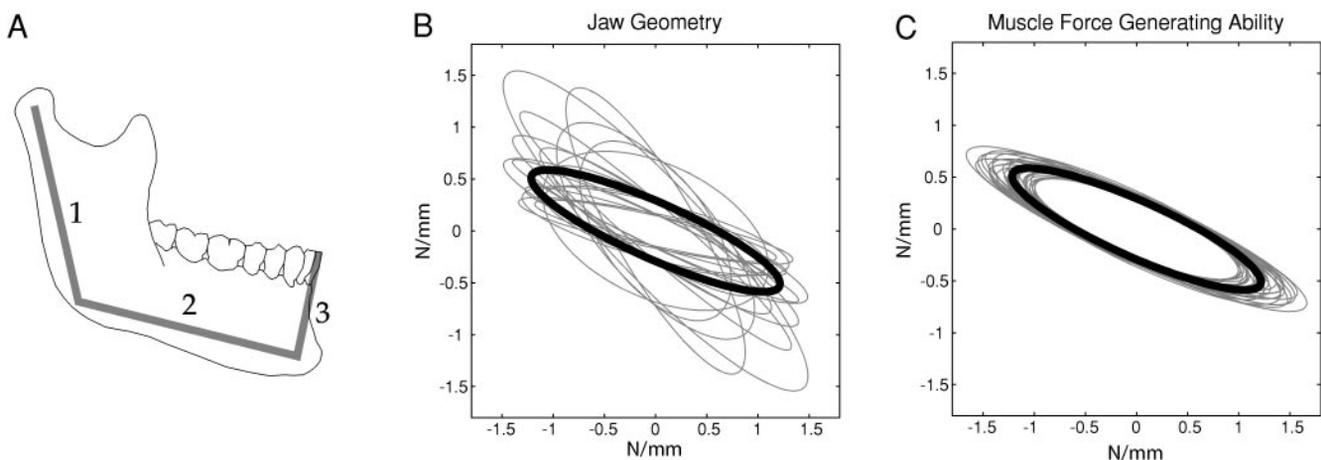


FIG. 11. *A*: schematic of modeled mandibular geometry showing the 3 manipulated segment lengths (see RESULTS). *B*: stiffness ellipses resulting from the manipulation of modeled jaw geometry. The dark ellipse shows stiffness under conditions of unaltered geometry. *C*: stiffness ellipses resulting from the random manipulation of muscle force-generating ability across all 7 muscles. The dark ellipse shows stiffness under unaltered conditions.

pronounced effect on the magnitude and orientation of the stiffness ellipse (Fig. 11*B*). Ellipse area was found to vary from −50.9 to +171.4% relative to the area obtained with unmodified jaw geometry. The orientation of the ellipse varied from −35.6 to +12.0° (a range of 47.6°).

We have in addition used the model to examine the effects of changing the relative balance of force-generating ability across the modeled muscles. In the model, muscle force-generating ability ($\rho$ in *Eq. 7*) is based on empirical estimates of maximum muscle force and physiological cross-sectional area and acts to scale muscle force output including resistance to stretch. Differences in force-generating ability across muscles may contribute to the observed asymmetries in the jaw-stiffness ellipse.

In the present simulations, we tested this idea by modifying the force-generating ability of modeled muscles in the range of −50 and +100%. This was done both for each muscle independently and by randomly varying the force-generating ability of all muscles simultaneously. The manipulation of modeled force-generating ability was found to affect the area of the stiffness ellipse but only had a small effect on ellipse orientation (Fig. 11*C*). The area of the stiffness ellipse varied from −23.8 to +62.1% relative to the area obtained using unaltered force-generating ability. Ellipse orientation varied from −3.0 to +2.5° (a range of 5.5°).

DISCUSSION

Jaw stiffness in the sagittal plane has been shown to have a nonuniform spatial distribution with greatest stiffness observed in the direction of protrusion and retraction. Consistent with the idea that speech movements reflect directional asymmetries in jaw stiffness, a detailed relationship between kinematic variability and stiffness was observed. Kinematic variability was found to be high in directions in which stiffness was low and variability was low in directions in which stiffness was high. In addition, for jaw positions that were closer to occlusion, stiffness was greater and kinematic variability was less.

The observed patterns of jaw stiffness and kinematic variability were not specific to speech—similar patterns appeared in speech and nonspeech conditions. This raises the possibility that the relationship between stiffness and variability is a general characteristic of orofacial function. Patterns of kinematic variation were also unaffected by differences in the direction of movement. For both jaw-opening and -protrusion movements, variability in position was greatest in the raising and lowering direction, that is, in directions in which stiffness is least.

Jaw stiffness was also estimated by simulating the experimental procedure using a model of the jaw. With the modeled control signals specifying jaw position held constant, the simulations yielded directional asymmetries in the stiffness ellipse that were similar to those observed empirically. The simulations were repeated with changes to muscle coactivation, to the relative levels of muscle force-generating ability and to the musculo-skeletal geometry of the jaw. Changes in the levels of muscle coactivation and muscle-force-generating ability affected the overall magnitude of jaw stiffness but had little effect on the orientation of the jaw-stiffness ellipse. Both the orientation and magnitude of the stiffness ellipse were significantly affected by changes in modeled jaw geometry. Thus both geometry and muscle force-generating ability affect stiffness, with jaw geometry dominating the orientation of the stiffness ellipse.

In the empirical study, stiffness magnitudes were greater for higher jaw positions. In the simulations, stiffness varies if the magnitude of the cocontraction command is changed. This result suggests that subjects may use higher levels of contraction for jaw positions closer to occlusion. This is consistent with the observation that muscle coactivation is a predominant characteristic of electromyographic activity in jaw muscles during speech (Moore et al. 1988).

Changes in stiffness may also arise as a consequence of position-dependent variation in reflex excitability in jaw muscles. In response to perturbation, higher stretch reflex excitability would be expected to contribute to higher stiffness. However, patterns of reflex excitability may differ depending on whether the jaw is stationary or in motion. van der Bilt et al. (1997) assessed masseter stretch reflex excitability during different phases of repetitive jaw-opening and -closing movements. It was found that reflex sensitivity was highest at the onset of the closing phase (lowest jaw elevation) and progressively decreased during jaw closing. Thus the contribution of jaw-closer reflexes to stiffness is presumably greatest at the initiation of the closing phase. In statics, a different pattern of jaw stretch reflex excitability has been observed. Fukuyama et al. (2000) examined masseter electromyographic activity in response to mechanical perturbations that were delivered at various jaw elevations while subjects maintained different levels of bite force. Higher levels of reflex activation were in general observed at jaw positions closer to occlusion. Although patterns of reflex excitability during speech production have yet to be assessed, the Fukuyama et al. (2000) results are consistent with the present finding that stiffness is greater at higher jaw elevations. Note, however, that regardless of the patterns of position-dependant changes to jaw stretch reflex excitability, measures of jaw stiffness are dependent on the relative balance of centrally specified coactivation and reflexes.

Measures of human jaw stiffness have been reported previously by Cooker et al. (1980) during maintained bite force. Stiffness levels of 10 N/mm were reported in response to 1.5-mm sinusoidal stretches in the direction of jaw raising and lowering while subjects maintained a mean bite force of 10 N. Higher stiffness (approximately 15 N/mm) was observed for smaller displacements, in the range of 0.2 mm. In the present study, stiffness levels in the raising and lowering direction were far lower, ranging from approximately 0.6 to 0.9 N/mm across the four vowel conditions. The higher values reported in the Cooker et al. (1980) study are presumably a reflection of the static bite force applied by subjects.

The present results bear on previous work in which it is suggested that kinematic variability in speech production is related to acoustical factors. Perkell and Nelson (1985) examined variability in the position of points along the tongue surface during the repeated production of vowels. Their findings suggested that kinematic variability is reduced in directions that have the greatest consequences for the acoustical outcome. In the present study, the pattern of kinematic variation is shown to be dependent on jaw geometry and jaw muscle properties. The dependence of variability in tongue movement on similar factors is unknown. However, the present findings underscore the importance of understanding the contribution of muscle mechanical and geometrical factors in the interpretation of patterns of kinematic variation.

Previous work on human arm movement suggests the possibil-

ity that the pattern of kinematic variability may be dependent simply on the direction of movement (Fitts 1954; Gordon et al. 1994; Harris and Wolpert 1998). In the present study, variability in jaw-raising and -lowering movements is indeed greater in the raising and lowering direction and less in the direction of protrusion and retraction. However, we have shown that kinematic variability is greatest in the direction of jaw raising and lowering even in the context of jaw-protrusion movements. Kinematic variability in the jaw is thus consistently related to the pattern of jaw stiffness not to the direction of movement.

We have observed a detailed relationship between the magnitude and orientation of patterns of jaw stiffness and kinematic variability. However, possible sources—other than stiffness—of the kinematic asymmetry observed here need to be considered. One possibility is that kinematic variation may also be related to other aspects of jaw impedance such as viscosity or inertia. In work on human arm movement, it has been difficult to obtain reliable estimates of viscosity and inertia because of the need to explicitly account for the contribution of dynamics to measured restoring forces. Indeed, any such estimation is dependent on an accurate model of the dynamics of the limb (Gomi and Kawato 1996). It would nevertheless be worthwhile to investigate approaches to the estimation of viscosity and inertia in the orofacial system and to likewise examine their relation to kinematic variability.

Stiffness of the human arm has been documented with the arm at rest (Flash and Mussa-Ivaldi 1990; Mussa-Ivaldi et al. 1985; Tsuji et al. 1995). The patterns of jaw stiffness observed in the present study differ in a number of respects from the patterns of stiffness at the hand. Whereas the orientation of the jaw-stiffness ellipse is essentially invariant with differences in jaw elevation, the orientation of the stiffness ellipse at the hand changes with workspace position. This might be explained by geometrical considerations in both cases. As the position of the hand varies in the horizontal plane, the major axis of the stiffness ellipse remains oriented toward the shoulder (Mussa-Ivaldi et al. 1985). The major axis of the jaw-stiffness ellipse similarly points toward the temporo-mandibular joint. The reason that differences in ellipse orientation are not observed in the jaw can be attributed to the relatively small range of angular jaw motion (typically 15° or less in speech).

REFERENCES

COOKER HS, LARSON CR, AND LUSCHEI ES. Evidence that the human jaw stretch reflex increases the resistance of the mandible to small displacements. *J Physiol (Lond)* 308: 61–78, 1980.

FELDMAN AG, ADAMOVICH SV, OSTRY DJ, AND FLANAGAN JR. The origin of electromyograms–explanations based on the equilibrium point hypothesis. In: *Multiple Muscle Systems: Biomechanics and Movement Organization,* edited by Winters J and Woo S. New York: Springer-Verlag, 1990, p. 195–213.

FITTS PM. The information capacity of the human motor system in controlling the amplitude of movement. *J Exp Psychol* 47: 381–391, 1954.

FLASH T. The control of hand equilibrium trajectories in multi-joint arm movements. *Biol Cybern* 57: 57–74, 1987.

FLASH T AND MUSSA-IVALDI F. Human arm stiffness characteristics during the maintenance of posture. *Exp Brain Res* 82: 315–326, 1990.

FUKUYAMA E, FUJITA Y, AND SOMA K. Changes in jaw-jerk on different levels of jaw closure and teeth-clenching in humans. *J Oral Rehabil* 27: 967–977, 2000.

GOMI H AND KAWATO M. Equilibrium-point control hypothesis examined by measured arm stiffness during multijoint movement. *Science* 272: 117–120, 1996.

GORDON JM, GHILARDI F, AND GHEZ C. Accuracy of planar reaching movements. I. independence of direction and extent. *Exp Brain Res* 99: 97–111, 1994.

GRIBBLE PL, OSTRY DJ, SANGUINETI V, AND LABOISSIÈRE R. Are complex control signals required for human arm movement? *J Neurophysiol* 79: 1409–1424, 1998.

HANNAM AG AND MCMILLAN AS. Internal organization in the human jaw muscles. *Crit Rev Oral Biol Med* 5: 55–89, 1994.

HARRIS CM AND WOLPERT DM. Signal-dependent noise determines motor planning. *Nature* 394: 780–784, 1998.

HELLSING G. Human jaw muscle motor behavior. I. Motor drive. *Swed Dent J* 11: 251–261, 1987.

KELSO JAS, VATIKIOTIS-BATESON E, SALTZMAN EL, AND KAY B. A qualitative dynamic analysis of reiterant speech production: phase portraits, kinematics, and dynamic modeling. *J Acoust Soc Am* 77: 266–280, 1985.

LABOISSIÈRE R, OSTRY DJ, AND FELDMAN AG. Control of multi-muscle systems: human jaw and hyoid movements. *Biol Cybern* 74: 373–384, 1996.

LUSCHEI ES AND GOLDBERG LJ. Neural mechanisms of mandibular control: mastication and voluntary biting. In: (Ed.), *Handbook of Physiology: The Nervous System.* Bethesda, MD: Am. Physiol. Soc., 1981, sect. 1, vol. II, p. 1237–1274.

MCDEVITT WE. *Functional Anatomy of the Masticatory System.* London, UK: Wright, 1989.

MCGRATH P AND MILLS P. *Atlas of Sectional Anatomy: Head, Neck, Trunk.* New York: Karger, 1984.

MILLS CM, GROOT DE J, AND POSIN JP. *Magnetic Resonance Imaging: Atlas of the Head, Neck, Spine.* Philedelphia, PA: Lea and Febiger, 1988.

MILNER T. Contribution of geometry and joint stiffness to mechanical stability of the human arm. *Exp Brain Res* 143: 515–519, 2002.

MOORE CA, SMITH A, AND RINGEL RL. Task-specific organization of activity in human jaw muscles. *J Speech Hear Res* 31: 670–80, 1988.

MULLER EM, MILENKOVIC PH, AND MACLEOD GE. Perioral tissue mechanics during speech production. *Proceedings of the Second IMAC International Symposium on Biomedical Systems Modeling,* edited by DeLisi C and Eisendfeld J. Amsterdam, North Holland, 1984.

MUSSA-IVALDI FA HOGAN N, AND BIZZI E. Neural, mechanical, and geometric factors subserving arm posture in humans. *J Neurosci* 5: 2732 2743, 1985.

OSTRY DJ, GRIBBLE PL, AND GRACCO VL. Coarticulation of jaw movements in speech production: is context-sensitivity in speech kinematics centrally planned? *J Neurosci* 16: 1570–1579, 1996.

OSTRY DJ AND MUNHALL KG. Control of rate and duration of speech movements. *J Acoust Soc Am* 77: 640–648, 1985.

OSTRY DJ, VATIKIOTIS-BATESON E, AND GRIBBLE PL. An examination of the degrees of freedom of human jaw motion in speech. *J Speech Lang Hear Res* 40: 1341–1351, 1997.

PERKELL JS AND NELSON WL. Variability in production of the vowels/i/and/a/. *J Acoust Soc Am* 77: 1889–1895, 1985.

PRUIM GJ, DE JONGH HJ, AND TEN BOSCH JJ. Forces acting on the mandible during bilateral static bite at different bite force levels. *J Biomech* 13: 755–763, 1980.

SCHEIDEMAN GB, BELL WH, LEGAN HL, FINN RA, AND REICH JS. Cephalometric analysis of dentofacial normals. *Am J Orthod* 78: 404–420, 1980.

SHILLER DM, GRIBBLE PL, AND OSTRY DJ. Effects of gravitational load on jaw movement in speech. *J Neurosci* 19: 9073–9080, 1999.

SHILLER DM, OSTRY DJ, GRIBBLE PL, AND LABOISSIÈRE R. Compensation for the effects of head acceleration on jaw movement in speech. *J Neurosci* 21: 6447–6456, 2001.

TRULSSON M AND JOHANSSON RS. Encoding of tooth loads by human periodontal afferents and their role in jaw motor control. *Prog Neurobiol* 49: 267–284, 1996.

TSUJI T, MORASSO PG, GOTO K, AND ITO K. Human hand impedance characteristics during maintained posture. *Biol Cybern* 72: 475–485, 1995.

VAN DER BILT A, OTTENHOFF FA, VAN DER GLAS HW, BOSMAN F, AND ABBINK JH. Modulation of the mandibular stretch reflex sensitivity during various phases of rhythmic open-close movements in humans. *J Dent Res* 76: 839–847, 1997.

VAN EIJDEN TM AND TURKAWSKI SJ. Morphology and physiology of masticatory muscle motor units. *Crit Rev Oral Biol Med* 12: 76–91, 2001.

WEIR J AND ABRAHAMS P. *An Atlas of Radiological Anatomy.* Kent, UK: Pitman Medical, 1978.

WOOD WW. A review of masticatory muscle function. *J Prosthet Dent* 57: 222–232, 1987.